Published in final edited form as:

Nano Lett. 2018 October 10; 18(10): 6500–6508. doi:10.1021/acs.nanolett.8b03032.

Predicting Nanotube Fibrogenicity through Stem Cell-Mediated Fibroblast Focus and Spheroid Formation

Xiaoqing He[†], **Chayanin Kiratipaiboon**[†], **Dale W. Porter**[‡], **Liying W. Rojanasakul**[‡], **Cerasela Zoica Dinu**[⊥], **Kai Wang**[§], **Yong Yang**[§], and **Yon Rojanasakul**[*,†,¶]

[†]Department of Pharmaceutical Sciences, West Virginia University, Morgantown, West Virginia 26506, United States

[‡]Health Effects Laboratory Division, National Institute for Occupational Safety and Health, Morgantown, West Virginia 26505, United States

[⊥]Department of Chemical Engineering, West Virginia University, Morgantown, West Virginia 26506, United States

[§]Department of Biomedical Engineering, University of North Texas, Denton, Texas 760207, United States

[¶]WVU Cancer Institute, West Virginia University, Morgantown, West Virginia 26506, United States

Abstract

Fibroblast stem cells or stemlike cells (FSCs) are proposed to play a pivotal role in extracellular matrix (ECM) regeneration by serving as a key source of ECM-producing fibro-blasts. We developed a mechanism-based in vitro model for fibrogenicity testing of nanomaterials based on their ability to induce FSCs. Using a FSC-enriched fibroblast focus model to mimic in vivo fibrogenic response, we demonstrated a dose-dependent increase in fibroblast focus formation and collagen production by primary lung fibroblasts treated with multiwalled carbon nanotubes (MWCNTs). The focus-forming cells exhibited stem properties as indicated by stem cell markers expression, sphere formation, and ALDH activity assays. Inhibition of ALDH activity diminished the focus and sphere formation as well as collagen production. In vivo animal studies supported the in vitro findings and indicated the potential utility of FSC-based assays as a rapid screening tool for fibrogenicity testing of nanomaterials. This study also unveils a novel mechanism of nanotube-induced fibrogenesis through ALDH-dependent FSC activation.

[*]**Corresponding Author:** Phone: 304-293-1476. Fax: 304-293 2576. yrojan@hsc.wvu.edu.

Author Contributions

X.H. conducted most experiments, analyzed data, and drafted the manuscript; C.K. conducted in vitro fibroblast stem cell experiments and analyzed data; D.W.P. conducted animal experiments and collected tissue samples; L.R. assisted with particle preparation and characterization; K.W. participated in imaging analysis; Y.Y. assisted with extracellular matrix measurements; C.Z.D. participated in particle characterization and preparation of the manuscript; YR coordinated and participated in all aspects of this study. All authors read and approved the final manuscript.

Supporting Information

The Supporting Information is available free of charge on the ACS Publications website at DOI: 10.1021/acs.nanolett.8b03032. Supplementary Figure S1: Characterization of MWCNTs showing transmission electron micrograph, Raman spectrum, X-ray photoelectron spectroscopy (XPS) survey scan spectrum and characteristics of MWCNTs. Supplementary Figure S2: Schematic diagram of MWCNT oropharyngeal aspiration in C57BL/6 J mice. Supplementary Figure S3: Immunofluorescence staining and quantification of collagen and OHdG in mouse lungs at 56 days. Supplementary experimental methods (PDF)

The authors declare no competing financial interest.

Graphical Abstract

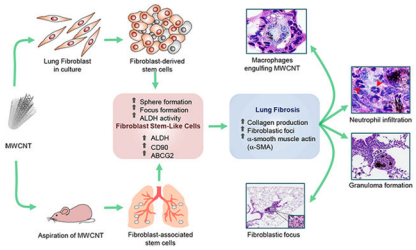

Keywords

Carbon nanotubes; fibrogenicity; fibroblasts; stem cells

Carbon nanomaterials including carbon nanotubes (CNTs) have increasingly been used for a wide array of applications in the fields as diverse as electronics, aerospace engineering, energy, and medicinal drug delivery. CNTs are built up of graphene sheets rolled into cylindrical structures with unique properties such as high tensile strength and durability with exceptional lightweight, making them attractive for various applications in structural and industrial engineering, energy storage, electronics, drug delivery and bioimaging.[1–4] CNTs have been shown to interact with cells and tissues in the body and with their increased utilization and production, there is a concern about their potential health risks, especially their long-term health risks such as fibrosis and cancer which are incurable at present. Understanding such risks will aid in the design of effective preventive measures and safe-by-design strategies for next-generation nanomaterials.

Experimental evidence indicates that CNTs can cause both acute and chronic adverse effects, especially to the respiratory system in animal models.[5–10] For example, pulmonary exposure to CNTs has been shown to induce acute inflammatory response,[5] activate cell death, and survival signaling pathways,[6–8] and cause pulmonary fibrosis.[9,10] However, contradictory results that showed no or minimal toxic effects of CNTs have also been reported.[11–13] In light of the lack of clear evidence for CNT pathogenicity, there is a great need to evaluate their health risks. CNTs are known to enter the lungs, penetrate alveolar epithelial barrier, and interact with specific lung cells such as macrophages and interstitial fibroblasts to induce fibroproliferation and ECM accumulation,[4,9,10] which are key hallmarks of lung fibrosis. Currently, most lung fibrosis studies have been conducted using animal models. However, such studies are costly and time-consuming; therefore, alternative test strategies that are more rapid and cost-effective are needed. Several in vitro models have been described, but their pathological relevance and reliability to predict the in vivo fibrogenic response remains an issue.

An important pathological feature of fibrosis is an accumulation of ECM that is clinically characterized by fibro-blast foci.[14,15] The presence and extent of this structure is one of the most reliable markers of poor prognosis in patients with fibrosis.[16,17] Animals studies also showed the induction of fibro-blast foci in the fibrotic lungs of mice treated with CNTs.[18] In this study, we developed a pathologically relevant in vitro model for rapid assessment of

CNT fibrogenicity based on their ability to induce fibroblast foci and spheroids in culture. Using primary human lung fibroblasts, we found that CNTs can induce fibroblast foci with a high level of collagen production, similar to that observed in vivo. Like fibroblast spheroids formed under stem cell-selective conditions, the fibroblast foci are enriched with FSCs, as evidenced by their stem cell markers expression and aldehyde dehydrogenase (ALDH) activity. Unlike the fibroblast foci previously reported by our group,[19] the foci described here do not depend on the use polylysine-coated glass substrate for focus formation; therefore the method is more reliable, rapid, and amendable to high throughput screening and coculture studies. Because FSCs are likely to be involved in the early stage of fibrosis, that is, by serving as a source of ECM-producing fibroblasts and myofibroblasts, we tested whether the FSC-based assays could be used as a predictive screening tool for fibrogenicity testing of nanomaterials. This study was conducted to test this feasibility and to evaluate the potential mechanisms of CNT-induced fibrosis through FSC activation.

Results and Discussion.

Nanomaterial Characterization.

The MWCNTs used in this study were characterized as previously described by Porter et al. [20] with 20–50 walls per nanotube and with minimal trace metal contamination, including sodium (0.41%) and iron (0.32%). Transmission electron microscopic analysis (Figure S1A,D) showed that the CNTs had an average length and width of 5.3 ± 2.0 μm and 80 ± 19 nm, respectively. Raman spectroscopy (Figure S1B,D) detected a typical carbon lattice structure with peaks at around 1358, 1590, and 2700 cm^{-1} and were assigned to the D-band, G-band, and 2D (G0)-band, respectively. A D-band to G-band intensity ratio of 0.132 was obtained, indicating of the structural integrity of the graphitic carbon lattice. The XPS survey scan (Figure S1C) revealed the existence of major carbon peak with no detectable other elements. Zeta potential measurements of MWCNTs were performed in water and in fibroblast cell culture medium (FBM) with 2% fetal bovine serum (FBS). In water, the values were −27.6 ± 0.3 mV, and in FBM with FBS (pH 7.6), the values were −10.5 ± 0.5 (Figure S1D).

MWCNTs Induce Fibroblast Focus Formation and Collagen Production.

The effects of MWCNTs on cell viability and proliferation of normal human lung fibroblasts (NHLFs) was first assessed in a standard 2D culture by MTS assay, which measures the reduction of tetrazolium substrate by viable cells to generate a colored formazan product. The cells were treated with MWCNTs at the surface area concentrations of 0, 0.04,0.08, 0.16, 0.32, 0.64, and 1.28 $\mu g/cm^2$ for 1 and 3 days. The in vitro concentration range of MWCNTs used in this study were estimated based on previous in vivo study showing the fibrogenic response at 40–80 μg of MWCNT aspiration in mice.[10] Dividing the in vivo dose by the average surface area of mouse lungs (approximately 500 cm^2)[21] indicates an equivalent in vitro surface area dose of 0.08–0.16 $\mu g/cm^2$. Moreover, this concentration range was chosen to include the low-dose physiologically relevant concentrations of CNTs[19,22,23] as well as the high cytotoxic concentrations to study the dose effects of CNTs. The results showed that at low concentrations (<0.16 $\mu g/cm^2$), the CNTs induced a slight but insignificant increase in cell proliferation, whereas at higher concentrations (>0.16 $\mu g/cm^2$)

they inhibited cell proliferation and caused cytotoxicity (Figure 1A). We then assessed the effect of MWCNTs on collagen production in the treated cells by immunoblotting. The results showed that the CNTs had a weak stimulatory effect on collagen expression at low concentrations (0.04–0.16 $\mu g/cm^2$) but a significant inhibitory effect at high concentration (0.32 $\mu g/cm^2$), likely due to cytotoxicity (Figure 1B). Next, we analyzed the dose effect of MWCNTs on fibroblast focus formation. NHLFs were treated with similar concentrations of MWCNTs and analyzed for focus formation by phase-contrast microscopy. As compared to standard cell proliferation assay, the focus formation assay showed a more pronounced dose effect of MWCNTs at the low-to-intermediate dose range of 0.02–0.16 $\mu g/cm^2$. At high doses (>1.28 $\mu g/cm^2$), the CNTs caused a cytotoxic effect (Figure 1C,D) producing less foci at 0.32 $\mu g/cm2$ and higher. The focus formation assay has commonly been used to evaluate the transforming capability of oncogenes and carcinogens in embryonic fibroblasts. In this study, we adapted this assay to evaluate the fibrogenic potential of CNTs in primary human lung fibroblasts. We found that this assay is more sensitive than the standard cell proliferation and collagen assays, which was further con-firmed in subsequent studies. Furthermore, this assay measures the ability of cells to form fibroblast foci, a structural feature that resembles the fibroblast foci in vivo which was confirmed in our animal study using the same CNTs.

We next evaluated the fibrogenic activity of focus-forming cells by analyzing collagen content in the cells isolated from the foci by immunoblotting and Sircol assays (Figure 1E–G). Our results showed that these cells were highly responsive to the stimulatory effect of CNTs as compared to the cells from normal cell culture treated with the same concentrations of CNTs. These results indicate that unlike the standard cell proliferation and collagen assays which are relatively insensitive to the fibrogenic effects of CNTs, the focus formation assay provides a superior sensitivity of detection for CNT fibrogenicity, In clinical settings, the formation of fibroblast foci is often used as a prognostic marker for pulmonary fibrosis.[24–26] In cell biology, the focus formation involves proliferation of stem cells or progenitor cells followed by colony formation. However, unlike colony formation which often indicates a neoplastic or malignant stage of cells, focus formation is a fibrotic rather than malignant process. This is supported by our recent study showing that CNT-treated primary lung fibroblasts do not form colonies on soft agar,[22] which is often used to indicate the malignancy of cells in vitro. However, these cells can promote colony formation and tumorigenesis of cancer cells.[22] Together our results indicate the potential utility of the focus formation assay as a sensitive method to detect the fibrogenic potential of CNTs. In addition to its sensitivity and ease of quantitation, this assay is also amenable to high throughput screening and more advanced coculture studies. Moreover, its simplicity and modest technical requirements make it cost-effective and practical for fibrogenicity testing of a large number of nanomaterials. However, it is necessary to determine proper concentration range for each nanomaterial because each nanomaterial has different physicochemical properties that could affect their fibrogenicity.

MWCNTs Induce Focus-Forming Stem Cells.

We previously demonstrated that CNTs can induce epithelial and fibroblast stem-like cells,[20,22,23] however their role in fibrogenesis remains obscure. We tested the ability of

MWCNTs to induce FSCs by 3D sphere formation and ALDH activity assays. The sphere formation assay has frequently been used to identify stem cells based on their ability to self-renew and differentiate at the single cell level in vitro,[27] while the ALDH activity assay is commonly used as a stem cell marker for various cell types. Figure 2A,B shows that treatment of NHLFs with MWCNTs induced sphere formation as compared to untreated controls which formed much small cell aggregates. Flow cytometric analysis of ALDH activity by Aldefluor assay showed that the CNT-treated cells exhibited a significantly higher ALDH activity as compared to untreated control (Figure 2C,D). Various isoforms of ALDH have been identified in different cells and tissues, most notably ALDH1A1 which is highly expressed in embryonic tissues and adult stem cells from bone marrow, brain, and breast tissues.[28] In this study, we found that this enzyme is also highly expressed in MWCNT-treated lung fibro-blasts, both in vitro (Figure 2G,H) and in vivo (Figure 5C,D). Together, these results support the stem-inducing activity of MWCNTs and their ability to induce FSCs.

Using various stem cell markers, we further demonstrated by immunofluorescence staining that the MWCNT-induced fibro-blast foci expressed a high level of mesenchymal stem cell markers, including αSMA, CD90, ABCG2, and ALDH as compared to untreated controls (Figure 2E–H). Furthermore, inhibition of ALDH activity by a specific ALDH inhibitor, diethylaminobenzaldehyde (DEAB), strongly inhibited the focus formation (Figure 3A,B) as well as sphere formation (Figure 3C,D) induced by MWCNTs. We also investigated collagen content in the fibroblast foci by histological staining of the focus-forming cells with aniline blue and Sirius red. Figure 3E–H shows that there was a marked increase in the collagen level in these cells from MWCNT-treated fibroblast foci and that the ALDH inhibitor strongly inhibited this increase, suggesting the potential role of ALDH-associated stem cells in MWCNT-induced fibrogenesis. To substantiate this finding, we used fluorescence activated cell sorting (FACS) to isolate cells that expressed a high ($ALDH^{high}$) and low ($ALDH^{low}$) level of ALDH, and analyzed their collagen content as well as αSMA expression by histological and immunofluorescence staining. The results showed that the $ALDH^{high}$ cells expressed significantly higher collagen and αSMA levels compared to $ALDH^{low}$ cells (Figure 3I–L). These results substantiate the role of ALDH-associated stem cells in MWCNT-induced fibrogenesis. In addition to establishing the role of these cells, these results also indicate the possible new mechanism of fibrosis induction through the activation of ALDH, which has not been reported. This novel finding may have important implications in the development of mechanism-based biomarkers and rapid screening tools for fibrogenicity testing of nanomaterials.

MWCNTs Induce Granuloma Formation and Lung Fibrosis in Vivo.

To verify the observed in vitro findings, we conducted in vivo experiments assessing the effects of MWCNT aspiration on lung pathology and FSC markers expression in a mouse model. Mice were exposed to DM (vehicle control; *see* Supporting Information) or 40 μg of MWCNT by oropharyngeal aspiration (Figure S2). At 7 and 56 days after the exposure, mice were analyzed for lung histopathology (Figure 4A), collagen expression, oxidative DNA damage (Figure S3A–C), and stem cell markers expression (Figure 5A–D). Histological analyses of the exposed lung tissues showed that unlike the control air-exposed

lungs which exhibited well organized airspaces and thin-walled alveolar structures, the MWCNT-exposed lungs exhibited disorganized alveolar structures with massive cellular infiltrates and granuloma-like masses at 7 days postexposure. At 56 days postexposure, the granuloma structures subsided but alveolar wall thickening and fibroblast focus formation progressed in the MWCNT-exposed lungs as compared to control lungs (Figure 4A).

Trichrome and Sirius red staining were used to indicate collagen deposition in mouse lungs. Extensive collagen deposition was evident in the lungs of mice treated with MWCNTs compared to control lungs, especially at 56 days postexposure where enhanced blue (trichrome/aniline blue) and red (Sirius red) staining of the alveolar walls and fibroblast foci were clearly evident (Figure 4B–D). Direct detection of collagen deposition by immunofluorescence staining using collagen-specific antibody also supported the increased collagen deposition in MWCNT-exposed lungs (Figure S3A,B). Such exposure also induced oxidative stress as indicated by the increased expression of DNA damage marker 8-hydroxy-deoxyguanosine (OHdG) (Figure S3A,C). Together these results demonstrated MWCNT-induced lung damage and ECM remodeling with inflammatory granuloma formation occurring predominantly at 7 days and fibrosis at 56 days postexposure. MWCNTs can induce the release of proinflammatory factors by macrophages and epithelial cells within lung alveoli, resulting in recruitment and accumulation of inflammatory cells including neutrophils, macrophages, and lymphocytes (Figure 4A). These acute inflammatory responses have been shown to reach an apex by day 7 after pulmonary exposure.[29] Subsequently, the pathological effects transit to the chronic phase which results from pro-fibrotic mediators secreted by macrophages and epithelial cells, including transforming growth factor-β (TGF-β), platelet-derived growth factor (PDGF), and Interleukin-1 (IL-1).[29,30] IL-1 can also induce the release of TGF-β and PDGF, known as crucial profibrotic mediators, from these cells. PDGF is known to stimulate fibroblast proliferation and recruitment of both of fibroblasts and myofibroblasts which can be observed by focus formation in mouse lungs. TGF-β can induce myofibroblast differentiation and collagen production. Additionally, myofibroblasts have been shown to possess high capacity of extracellular matrix (ECM) protein synthesis and secretion, including collagen and fibronectin, during the chronic phase of fibrosis.[29,30] This results in deposition of ECM, exhibited by collagen deposition and alveolar wall thickening in mouse lungs (Figure 4A–D).

MWCNTs Induce Fibroblast-Associated Stem Cells in Vivo.

Lung tissue sections from MWCNT-exposed mice were analyzed for stem cell markers expression by Immunofluorescence staining. CD90, a lung mesenchymal stem cell marker, was found to be highly upregulated in the MWCNT-exposed lungs at 7 days postexposure. At 56 days, the level of this marker declined but was still higher than that in the control group. α-Smooth muscle actin (αSMA), a myofibroblast marker, was also increased after 7 and 56 days (Figure 5A,B). Likewise, ALDH and ABCG2, general stem cell markers, were highly upregulated in the MWCNT-exposed lungs versus control lungs, both at 7 and 56 days after the exposure (Figure 5C,D). These results are consistent with the in vitro findings and indicated an upregulation of fibroblast-associated stem cell markers in the fibrotic lungs of mice treated with MWCNTs. Because of their self-renewal property, as demonstrated by

sphere formation assay, these cells could serve as a source of collagen-producing fibroblasts or myofibroblasts that contribute to fibrosis.

Conclusions.

In this study, we reported a rapid and sensitive in vitro assay for fibrogenicity testing of carbon nanoubes, which may be applicable to other nanomaterials. The assay is based on the ability of primary lung fibroblasts to form FSC-enriched fibroblast foci and spheres in culture. The foci and spheres formed by MWCNT-treated cells expressed a high level of collagen similar to that observed in the fibroblast foci of patients with pulmonary fibrosis.[20] The MWCNT-induced foci and spheres also expressed a high level of mesenchymal or fibroblast-associated stem cell markers including CD90, αSMA, ABCG2, and ALDH, suggesting the role of FSCs in MWCNT-induced fibrogenesis. In vivo animal studies support the in vitro findings and indicate the induction of lung fibrosis and fibroblast-associated stem cells by MWCNTs. Mechanistic studies revealed ALDH as a key stem cell regulator of MWCNT-induced fibrogenesis. Our findings support the potential utility of FSC-based focus and sphere formation assays as rapid screening tools for fibrogenicity testing of nano-materials and unveil a novel mechanism of MWCNT-induced fibrosis through the activation of ALDH-associated FSCs.

Supplementary Material

Refer to Web version on PubMed Central for supplementary material.

ACKNOWLEDGMENTS

This work was supported by grants from the National Institutes of Health (R01-EB018857, R01-ES022968, and R15-GM122953) and National Science Foundation (CBET-1434503). We thank Dr. Kathleen Brundage for the support with flow cytometry analysis and Emily Ellis for animal experiments. Flow cytometry experiments were performed in the West Virginia University Flow Cytometry Core Facility, which is supported by the National Institute of Health equipment Grant S10OD16165 and the Institutional Development Award (IDeA) from the National Institute of General Medical Sciences of the National Institutes of Health through Grants P30GM103488 (CoBRE) and P20GM103434 (INBRE). The findings and conclusions in this report are those of the author(s) and do not necessarily represent the official position of the National Institute for Occupational Safety and Health, Centers for Disease Control and Prevention.

REFERENCES

(1). De Volder MF; Tawfick SH; Baughman RH; Hart AJ Carbon Nanotubes: Present and Future Commercial Applications. Science 2013, 339, 535–539. [PubMed: 23372006]

(2). Schnorr JM; Swager TM Emerging Applications of Carbon Nanotubes. Chem. Mater 2011, 23, 646–657.

(3). Luanpitpong S; Wang L; Davidson DC; Riedel H; Rojanasakul Y Carcinogenic Potential of High Aspect Ratio Carbon Nanomaterials. Environ. Sci.: Nano 2016, 3, 483–493. [PubMed: 27570625]

(4). Luanpitpong S; Wang L; Rojanasakul Y The effects of carbon nanotubes on lung and dermal cellular behaviors. Nanomedicine (London, U. K.) 2014, 9, 895–912.

(5). Huizar I; Malur A; Midgette YA; Kukoly C; Chen P; Ke PC; Podila R; Rao AM; Wingard CJ; Dobbs L; Barna BP; Kavuru MS; Thomassen MJ Novel Murine Model of Chronic Granulomatous Lung Inflammation Elicited by Carbon Nanotubes. Am. J. Respir. Cell Mol. Biol 2011, 45, 858–866. [PubMed: 21398620]

(6). He X; Young S; Schwegler-Berry D; Chisholm WP; Fernback JE; Ma Q Multiwalled carbon nanotubes induce a fibrogenic response by stimulating reactive oxygen species production, activating NF-kB signaling, and promoting fibroblast-to-myofibroblast transformation. Chem. Res. Toxicol 2011, 24, 2237–2248. [PubMed: 22081859]

(7). Azad N; Iyer AK; Wang L; Liu Y; Lu Y; Rojanasakul Y Reactive Oxygen Species-Mediated p38 MAPK Regulates Carbon Nanotube-Induced Fibrogenic and Angiogenic Responses. Nanotoxicology 2013, 7, 157–168. [PubMed: 22263913]

(8). Wang P; Nie X; Wang Y; Li Y; Ge C; Zhang L; Wang L; Bai R; Chen Z; Zhao Y; Chen C Multiwall Carbon Nanotubes Mediate Macrophage Activation and Promote Pulmonary Fibrosis through Tgf-Beta/Smad Signaling Pathway. Small 2013, 9, 3799–3811. [PubMed: 23650105]

(9). Wang X; Xia T; Ntim SA; Ji Z; Lin S; Meng H; Chung CH; George S; Zhang H; Wang M; Li N; Yang Y; Castranova V; Mitra S; Bonner JC; Nel AE Dispersal State of Multiwalled Carbon Nanotubes Elicits Profibrogenic Cellular Responses That Correlate with Fibrogenesis Biomarkers and Fibrosis in the Murine Lung. ACS Nano 2011, 5, 9772–9787. [PubMed: 22047207]

(10). Mercer RR; Hubbs AF; Scabilloni JF; Wang L; Battelli LA; Friend S; Castranova V; Porter DW Pulmonary Fibrotic Response to Aspiration of Multi-Walled Carbon Nanotubes. Part. Fibre Toxicol 2011, 8, 21. [PubMed: 21781304]

(11). Albanese A; Tang PS; Chan WC The Effect of Nanoparticle Size, Shape, and Surface Chemistry on Biological Systems. Annu. Rev. Biomed. Eng 2012, 14, 1–16. [PubMed: 22524388]

(12). Stoeger T; Reinhard C; Takenaka S; Schroeppel A; Karg E; Ritter B; Heyder J; Schulz H Instillation of Six Different Ultrafine Carbon Particles Indicates a Surface Area Threshold Dose for Acute Lung Inflammation in Mice. Environ. Health Perspect 2006, 114, 328–333. [PubMed: 16507453]

(13). Wang L; Stueckle TA; Mishra A; Derk R; Meighan T; Castranova V; Rojanasakul Y Neoplastic-like Transformation Effect of Single-walled and Multi-walled Carbon Nanotubes Compared to Asbestos on Human Lung Small Airway Epithelial Cells. Nanotoxicology 2014, 8, 485–507. [PubMed: 23634900]

(14). Cha SI; Groshong SD; Frankel SK; Edelman BL; Cosgrove GP; Terry-Powers JL; Remigio LK; Curran-Everett D; Brown KK; Cool CD; Riches DW Compartmentalized Expression of c-FLIP in Lung Tissues of Patients with Idiopathic Pulmonary Fibrosis. Am. J. Respir. Cell Mol. Biol 2010, 42, 140–148. [PubMed: 19372246]

(15). Harada T; Watanabe K; Nabeshima K; Hamasaki M; Iwasaki H Prognostic Significance of Fibroblastic Foci in Usual Interstitial Pneumonia and Non-specific Interstitial Pneumonia. Respirology 2013, 18, 278–283. [PubMed: 23016880]

(16). Meuten T; Hickey A; Franklin K; Grossi B; Tobias J; Newman DR; Jennings SH; Correa M; Sannes PL WNT7B in Fibroblastic Foci of Idiopathic Pulmonary Fibrosis. Respir. Res 2012, 13, 62. [PubMed: 22838404]

(17). Lomas NJ; Watts KL; Akram KM; Forsyth NR; Spiteri MA Idiopathic Pulmonary Fibrosis: Immunohistochemical Analysis Provides Fresh Insights into Lung Tissue Remodelling with Implications for Novel Prognostic Markers. Int. J. Clin. Exp. Pathol 2012, 5, 58–71. [PubMed: 22295148]

(18). Dong J; Ma Q Osteopontin Enhances Multi-walled Carbon Nanotube-Triggered Lung Fibrosis by Promoting TGF-β1 Activation and Myofibroblast Differentiation. Part. Fibre Toxicol 2017, 14, 18. [PubMed: 28595626]

(19). Luanpitpong S; Wang L; Manke A; Martin KH; Ammer AG; Castranova V; Yang Y; Rojansakul Y Induction of Stem-like Cells with Fibrogenic Properties by Carbon Nanotubes and Its Role in Fibrogenesis. Nano Lett 2014, 14, 3110–3116. [PubMed: 24873662]

(20). Porter DW; Hubbs AF; Mercer RR; Wu N; Wolfarth MG; Sriram K; Leonard S; Battelli L; Schwegler-Berry D; Friend S; Andrew M; Chen BT; Tsuruoka S; Endo M; Castranova V Mouse pulmonary dose- and time course-responses induced by exposure to multi-walled carbon nanotubes. Toxicology 2010, 269, 136–147. [PubMed: 19857541]

(21). Stone KC; Mercer RR; Gehr P; Stockstill B; Crapo JD Allometric Relationships of Cell Numbers and Size in the Mammalian Lung. Am. J. Respir. Cell Mol. Biol 1992, 6, 235–243. [PubMed: 1540387]

(22). Luanpitpong S; Wang L; Castranova V; Dinu CZ; Issaragrisil S; Chen YC; Rojanasakul Y Induction of Cancer-Associated Fibroblasts by Carbon Nanotubes Dictates its Tumor-igenicity. Sci. Rep 2016, 6, 39558. [PubMed: 27996035]

(23). Luanpitpong S; Wang L; Castranova V; Rojanasakul Y Induction of Stem-like Cells with Malignant Properties by Chronic Exposure of Human Lung Epithelial Cells to Single-Walled Carbon Nanotubes. Part. Fibre Toxicol 2014, 11, 22. [PubMed: 24885671]

(24). Jones MG; Fabre A; Schneider P; Cinetto F; Sgalla G; Mavrogordato M; Jogai S; Alzetani A; Marshall BG; O'Reilly KM; Warner JA; Lackie PM; Davies DE; Hansell DM; Nicholson AG; Sinclair I; Brown KK; Richeldi L Three-Dimensional Characterization of Fibroblast Foci in Idiopathic Pulmonary Fibrosis. JCI Insight 2016, 1, e86375. [PubMed: 27275013]

(25). Meuten T; Hickey A; Franklin K; Grossi B; Tobias J; Newman DR; Jennings SH; Correa M; Sannes PL WNT7B in Fibroblastic Foci of Idiopathic Pulmonary Fibrosis. Respir Res 2012, 13, 62. [PubMed: 22838404]

(26). Scotton CJ; Chambers RC Molecular Targets in Pulmonary Fibrosis: the Myofibroblast in Focus. Chest 2007, 132, 1311–1321. [PubMed: 17934117]

(27). Pastrana E; Silva-Vargas V; Doetsch F Eyes Wide Open: a Critical Review of Sphere-Formation as an Assay for Stem Cells. Cell Stem Cell 2011, 8, 486–498. [PubMed: 21549325]

(28). Moreb JS Aldehyde Dehydrogenase as a Marker for Stem Cells. Curr. Stem Cell Res. Ther 2008, 3, 237–246. [PubMed: 19075754]

(29). Dong J; Ma Q Myofibroblasts and Lung Fibrosis Induced by Carbon Nanotube Exposure. Part. Fibre Toxicol 2016, 13, 60. [PubMed: 27814727]

(30). Vietti G; Lison D; van den Brule S Mechanisms of Lung Fibrosis Induced by Carbon Nanotubes: Towards an Adverse Outcome Pathway (AOP). Part. Fibre Toxicol 2015, 13, 11.

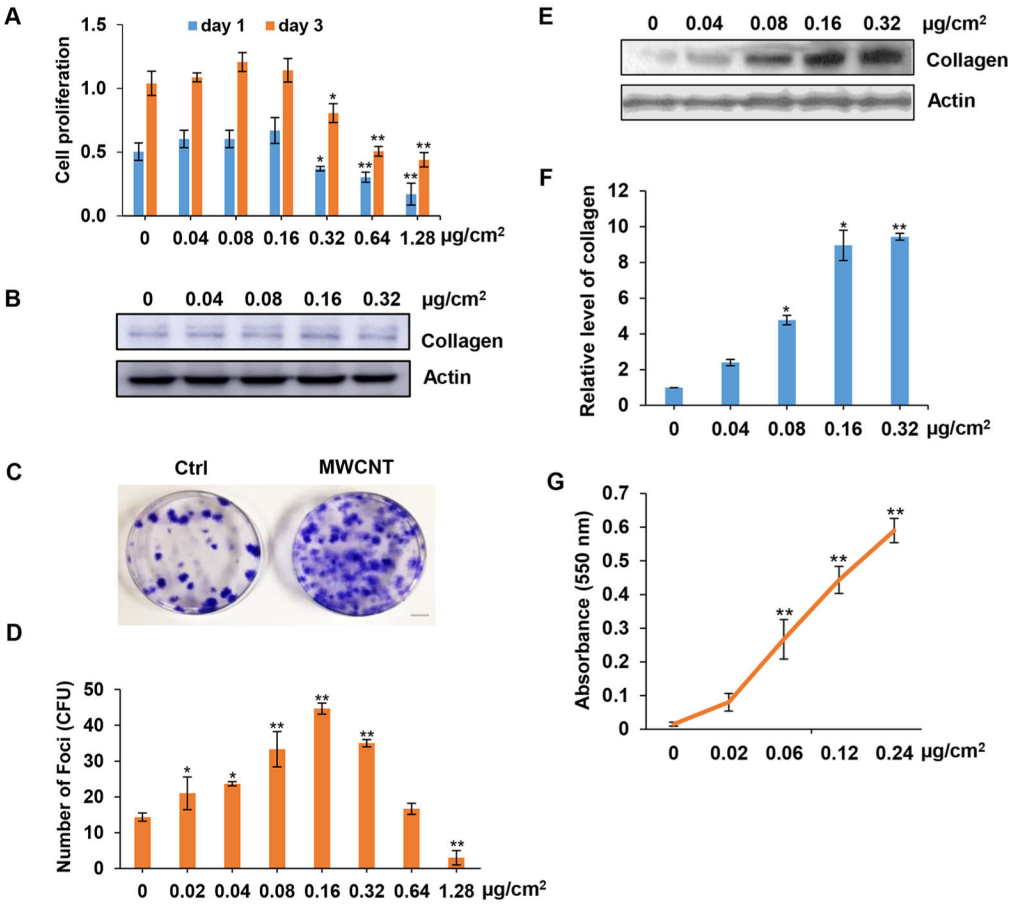

Figure 1.

MWCNTs induce focus formation and collagen production in primary human lung fibroblasts. (A) Proliferation of NHLFs grown in a standard 2D cell culture. The cells were treated with various concentrations of MWCNT and cell proliferation was determined by MTS assay at 1 and 3 days post-treatment. (B) Immunoblotting of collagen in MWCNT-treated cells. (C) Representative images of focus formation in cells treated with 0.16 μg/cm^2 MWCNT. Fibroblast foci were formed under a low seeding density of 2.5×10^3 cells/well in 6-well plates. Images were taken at 14 days post-treatment. (D) Dose dependent effect of MWCNT on focus formation. (E,F) Immunoblotting of collagen production in MWCNT-treated focus-forming cells. (G) Detection of collagen production by Sircol assay in focus-forming cells. *$p < 0.05$, **$p < 0.001$ versus Ctrl, $n = 4$.

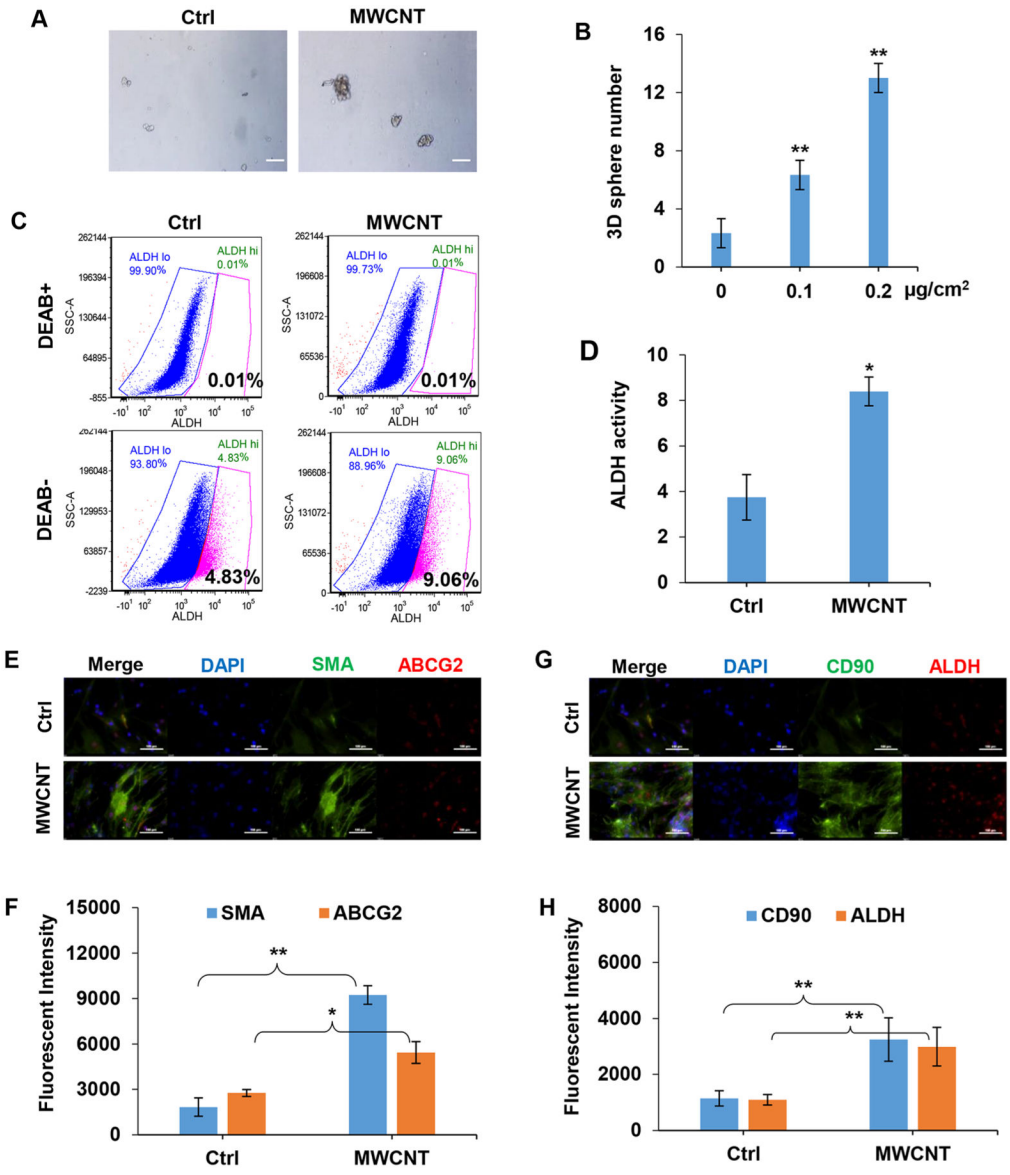

Figure 2.

MWCNTs induce stem-like cells in NHLFs. (A) The 3D spheres formed by NHLFs treated with 0.16 μg/cm^2 MWCNT for 14 days under nonadherent conditions. Scale bar is 100 μm. (B) Quantitation of 3D spheres with size larger than 20 μm in diameter. (C) Flow cytometry graphical representation of ALDH activity in MWCNT-treated cells with or without DEAB, an ALDH inhibitor, which was used as an internal control for baseline ALDH activity measurements. (D) Quantification of ALDH activity, means ± s.d. (n = 3), *p < 0.05. (E,F) Immunofluorescence staining and quantification of αSMA and ABCG2 in MWCNT-induced fibroblast foci. Scale bar is 100 μm. (G,H) Immunofluorescence staining and quantification of CD90 and ALDH in MWCNT-induced fibroblast foci using image analysis software. Scale bar is 100 μm. *$p < 0.05$, **$p < 0.001$ versus Ctrl, $n = 3$.

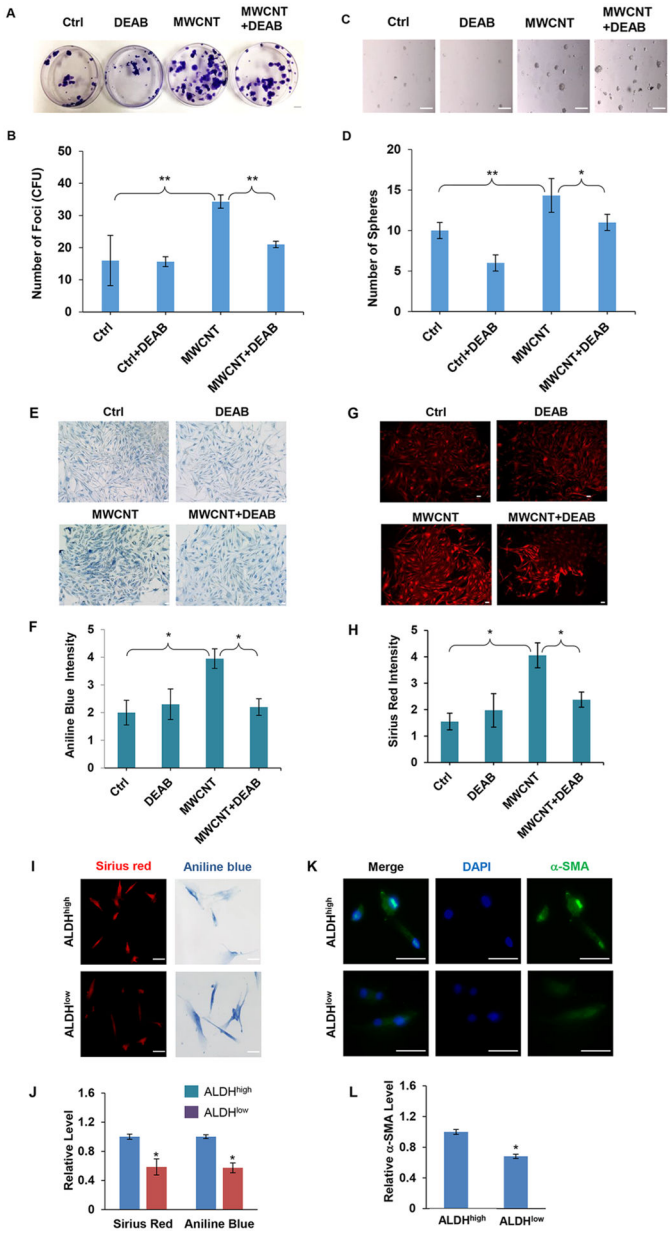

Figure 3.

ALDH inhibitor DEAB inhibits MWCNT-induced focus and sphere formation and ALDH regulates fibrogenic activity of MWCNT-treated lung fibroblasts. (A) Representative images and (B) quantification of focus formation in control and MWCNT-treated NHLFs. Cells were treated with MWCNT (0.16 μg/cm^2) in the presence or absence of DEAB (50 μM) for 14 days and analyzed for focus formation.(C) Representative images and (D) quantification of sphere formation in control and MWCNT-treated NHLFs. Cells were similarly treated with the test agents and allowed to grow under nonadherent, stem cell-selective conditions for 14 days and analyzed for sphere formation. Scale bar is 100 μm. *$p < 0.05$, **$p < 0.001$ versus Ctrl, $n = 3$. (E–H) Representative images and quantification of collagen content in focus-forming cells stained with Trichrome (aniline blue) and Sirius red. NHLFs were

treated with MWCNT (0.16 μg/cm^2) in the presence or absence of DEAB (50 μM) for 14 days and analyzed for collagen content. Scale bar is 100 μm. (I,J) Representative images and quantification of collagen content in sorted ALDH^{high} and ALDH^{low} cells. NHLFs were treated with MWCNT (0.16 μg/cm^2) for 72 h and analyzed for ALDH activity by flow cytometry-based Aldeflour assay. The cells were sorted by FACS and analyzed for collagen content by aniline blue and Sirius red staining. Scale bar is 100 μm. (K,L) Representative images and quantification of αSMA expression in the sorted cells stained with αSMA antibody by immunofluorescence. Quantitation of staining was performed using an image analysis software. Scale bar is 50 μm. *$p < 0.05$ versus Ctrl, $n = 3$.

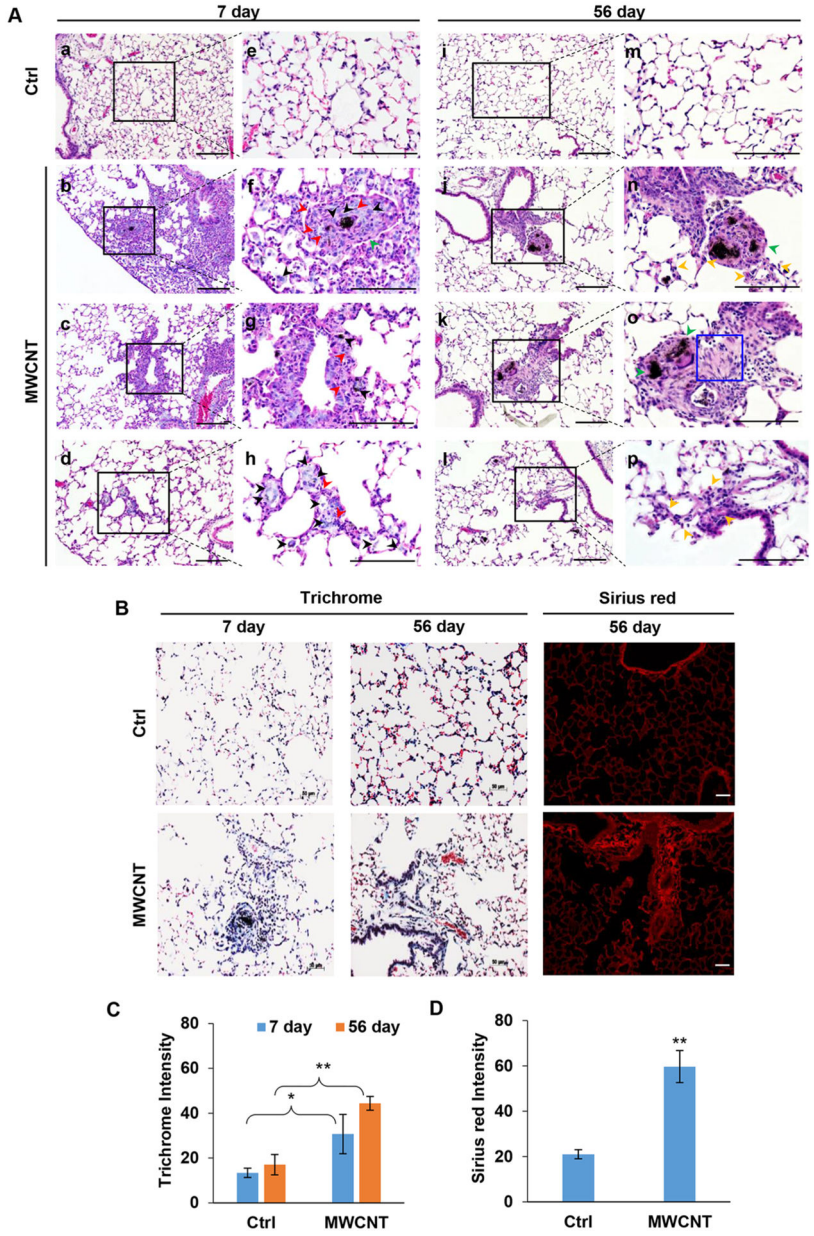

Figure 4.

Effects of MWCNT lung exposure in mice. (A) H&E staining of lung tissue sections from mice exposed to 0 or 40 μg MWCNT at 7 days (a–h) and 56 days (i–p) postexposure (a–d and i–l, at 20× magnification; e–h and m–p, at 40× magnification). Deposition of MWCNTs is visible as black spots on the tissue sections. Black, red, green, and yellow arrow heads indicate macrophages, neutrophils, granuloma formation, and alveolar wall thickening, respectively. Blue box denotes fibroblast focus. (B) Trichrome and Sirius red staining of MWCNT-exposed mouse lungs at 7 and 56 days postexposure. (C,D) Quantitative analysis of Trichrome and Sirius red staining. Quantitation of staining was performed using an image analysis software. Scale bar is 100 μm. *$p < 0.05$, **$p < 0.001$ versus Ctrl, $n = 3$.

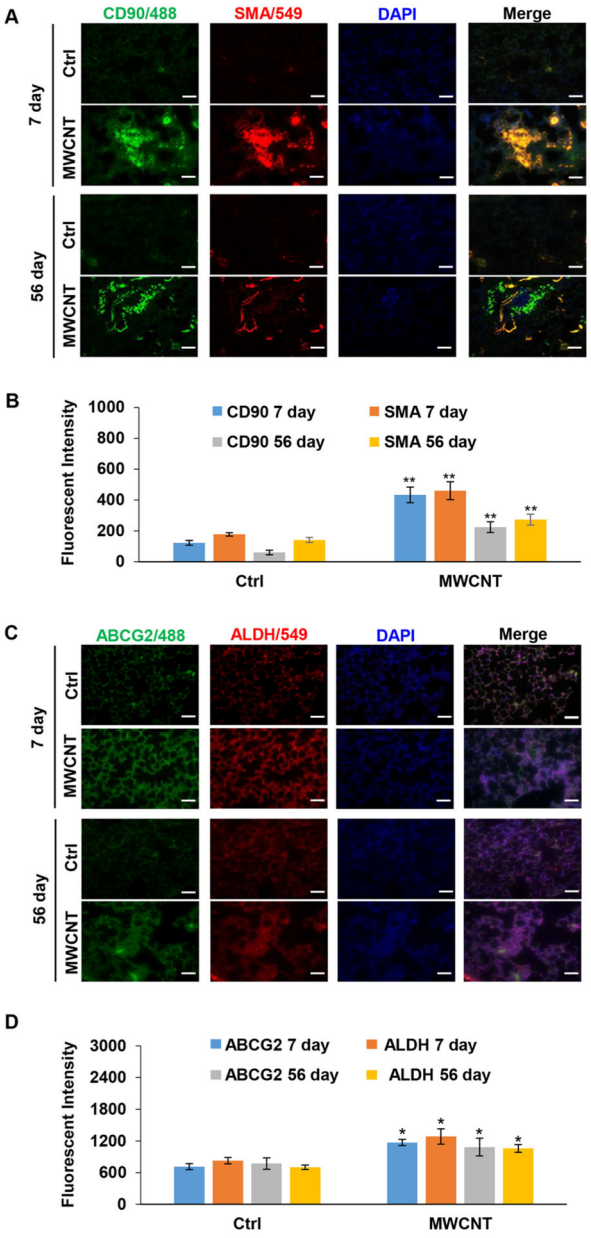

Figure 5.

MWCNT exposure upregulates stem cell markers in mouse lungs. (A,B) Immunofluorescence staining and quantification of CD90 and αSMA in mouse lungs. (C,D) Immunofluorescence staining and quantification of ABCG2 and ALDH in mouse lungs. Exposure was performed as described in Figure 4 Scale bar is 100 μm. *$p < 0.05$, **$p < 0.001$ versus Ctrl, $n = 3$.